Environmental Science and Pollution Research (2021) 28:22602–22611
https://doi.org/10.1007/s11356-020-11928-0

RESEARCH ARTICLE

High leaf area index inhibits net primary production in global temperate forest ecosystems

Wei Zhao [1,2] · Wenfeng Tan [2,3] · Shiqing Li [1,2]

Received: 7 September 2020 / Accepted: 1 December 2020 / Published online: 9 January 2021

Abstract

Within limited growth age in some regions, forest production, including gross primary production (GPP) and net primary production (NPP), was linearly correlated with leaf area index (LAI). However, over wide range of growth age in the global scale, LAI patterns of forest production are unclear. Here, we compiled a subset from the Global Soil Respiration Database (SRDB) for global temperate forest ecosystems. The subset database mainly included forest production, soil respiration, and LAI data in 493 study sites over wide range of forest growth age (0–500 years). The results showed that LAI initially increased rapidly, reached a peak at juvenility, decreased slowly until maturity, and again increased possibly with further forest aging (R^2 = 0.21, $P < 0.001$). We found that the dynamics of both GPP and NPP across global temperate forest ecosystems were driven by LAI. GPP initially increased and subsequently stabilized with increasing LAI. NPP peaked at LAI of about 5.6 m^2 m^{-2}, and subsequently decreased. The decrease in NPP resulted from the asymptotic increase in GPP and the continuing decrease in the NPP/GPP ratio with increasing LAI. The decline in the NPP/GPP ratio resulted from the significant increase in autotrophic respiration (R_a), and especially after canopy closure, R_a increased more quickly with increasing LAI than GPP. These results will improve our understanding of the control of LAI on ecosystem production.

Keywords Vegetation structure · Canopy photosynthesis · Plant respiration · Carbon use efficiency · Ecosystem development · Temperate forest production

Introduction

Patterns of forest production with age and their determinants have been extensively investigated (Gower et al. 1996; Ryan et al. 1997; Pregitzer and Euskirchen 2004; He et al. 2012; Tang et al. 2014). Forest production covers gross primary production (GPP) and net primary production (NPP). Forest aboveground net primary production (ANPP) is considered to increase during initial growth, peaks at maturity, and then gradually decreases with forest age (Gower et al. 1996; Ryan et al. 1997; Pregitzer and Euskirchen 2004; Ryan et al. 2004; Luyssaert et al. 2008; Drake et al. 2011; He et al. 2012; Kashian et al. 2013), whereas gross primary production (GPP) remains quasi-constant (Fig. S1). Process and causes of age-related changes in regional forest production have been discussed much based on nutrient supply and plant physiology (Gower et al. 1996; Ryan et al. 1997); however, explanation of plant canopy structure to changes in global temperate forest production has been rarely reported.

The plant canopy is a place of physical and biogeochemical processes in an ecosystem. The functional and structural features of plant canopies are influenced by microclimatic environment, nutrient dynamics, and many other factors (de Almeida et al. 2019; da Silva et al. 2020; Han et al. 2020). The integrated effect of these factors on plant canopies is reflected by the amount and area of foliage (Parker 2020). Consequently, canopy leaf area acts as the important control over primary production (photosynthesis), respiration,

Responsible Editor: Philippe Garrigues

✉ Wei Zhao
aoei@nwafu.edu.cn

[1] State Key Laboratory of Soil Erosion and Dryland Farming on the Loess Plateau, Northwest A&F University, Yangling 712100, People's Republic of China

[2] Institute of Soil and Water Conservation, Chinese Academy of Sciences and the Ministry of Water Resources, Yangling 712100, People's Republic of China

[3] College of Resources and Environment, Huazhong Agricultural University, Wuhan 430070, People's Republic of China

transpiration, and other physiological attributes related to ecosystem processes (Fotis et al. 2018; Kulmala et al. 2019; Li et al. 2020; Wales et al. 2020). The leaf area index (LAI) is an indicator of the canopy leaf surface and defined as one half the total green leaf area (m^2) per unit horizontal ground surface (m^2). LAI, acting as characteristic of vegetation structure, has become an important parameter in ecological field and modeling studies (Sellers et al. 1988; Sellers et al. 1997; Bondeau et al. 1999; Lee et al. 2019).

Some studies have reported that the vegetation structure, LAI, can satisfactorily explain the variation in forest production (Asner et al. 2003; Kushida et al. 2007; Zha et al. 2013). At an individual tree-species level, Kushida et al. (2007) found that the larch forest NPP was significantly, linearly, and positively correlated with LAI, and 90% of the variation in larch NPP was explained by LAI. Based on 18 forest stand studies representing 5–123 years of growth in Canada, Zha et al. (2013) also found that the leaf area index was positively correlated with forest production and can explain 66–80% of the variation in forest production. However, in these studies, the single tree species studied in a regional scope (Kushida et al. 2007) or the limited forest age (< 170 years; Kushida et al. 2007; Zha et al. 2013) will result in some uncertainties in the global relationship between forest production and LAI. At global scale, Asner et al. (2003) found that 33% of the variation in ANPP could be explained by LAI; however, the global relationship between forest NPP and LAI is unclear. Because ANPP only accounted for 53–77% of NPP (Gower et al. 1992), belowground net primary production (BNPP; root production) comprising a large proportion of NPP (23–47%) will lead to some uncertainty in the global relationship between forest NPP and LAI. Here, BNPP is the difference between belowground GPP and root respiration (Luyssaert et al. 2007).

About 25% of the world's forests are in the temperate biome (Tyrrell et al. 2012); thus, understanding the control of LAI on ecosystem production of temperate forests is necessary to improve our ability to predict long-term ecosystem responses to global change for making sound climate change policies. Deciphering the linkage between temperate forest age and LAI can clarify the role of forest age as an important variable in ecosystem models. Therefore, we compiled a subset of global natural temperate forest dataset from the recently assembled extensive Global Soil Respiration Database (Bond-Lamberty and Thomson 2018) to (i) determine the dynamics of LAI (0–15 m^2 m^{-2}) with long-term forest growth (0–500 years), and (ii) determine LAI-driven patterns of forest production.

Materials and methods

The database used in our study was compiled from version v20191103a of the Global Soil Respiration Database (SRDB; Bond-Lamberty and Thomson 2018), downloaded on 21 November 2019 from https://github.com/bpbond/srdb. The SRDB was assembled from published literature. The published studies reported at least one of the following data measured in the field (not laboratory): annual soil respiration, mean seasonal soil respiration, a seasonal or annual partitioning of soil respiration into its source fluxes, soil respiration temperature response (Q10), or soil respiration at 10 °C. Therefore, there are few study sites including simultaneously GPP, NPP, net ecosystem production (NEP), root respiration, and heterotrophic respiration, and these variables are missing on different degrees for study sites. The SRDB is dominated by temperate, well-drained forest measurement locations. Version 4 of SRDB encompassed 1458 published studies with measurements taken between 1961 and 2016. These published studies included mainly 4396 forest, 1133 grassland, and 1084 agriculture ecosystems. We compiled a subset of the database derived from SRDB by using geography (latitude, longitude), GPP, NPP, net ecosystem production (NEP), root respiration, heterotrophic respiration (R_h), leaf area index (LAI), and age (years since regeneration after a major disturbance, e.g., harvest and fire). We excluded any forest sites subject to artificial treatments (e.g., fertilization, drought treatment, elevated ambient CO_2 concentration, and/or irrigation). We used CO_2 fluxes measured by infrared gas analyzers or gas chromatography, excluding soda lime measurements that may underestimate CO_2 fluxes. In our compiled subset database derived from the SRDB, 493 study sites of temperate forests were selected (Fig. 1).

We tested different functions to fit the data, including a linear function, a polynomial function, an exponential function, a logarithmic function, a gamma (Γ) function ($y = ax^b e^{cx}$, and a, b, and c are parameters; Tang et al. (2014)), a Michaelis–Menten function [$y = ax/(b + x)$, and a, b, and c are parameters], and a combination of two functions. The data were fitted by the Levenberg-Marquardt (LM) algorithm across global temperate forest ecosystems. The LM algorithm is an iterative technique, and can determine the minimum of a multivariate function that is expressed as the sum of squares of nonlinear real-valued functions (Levenberg 1944; Marquardt 1963). It has been considered as a standard technique for solving nonlinear least-squares problems (Lourakis 2005). We used the root-mean-squared error (RMSE) to assess the model accuracy and efficiency. In addition, we used the Akaike information criterion (AIC) to compare models as AIC considers the trade-off between goodness-of-fit (model explanatory) and the model complexity (number of parameters) (Migliavacca et al. 2012; Yang et al. 2012). When the number of parameters (p) is large compared with the sample size (n) (generally $n/p < 40$), we used the corrected AIC for the small sample (Migliavacca et al. 2012).

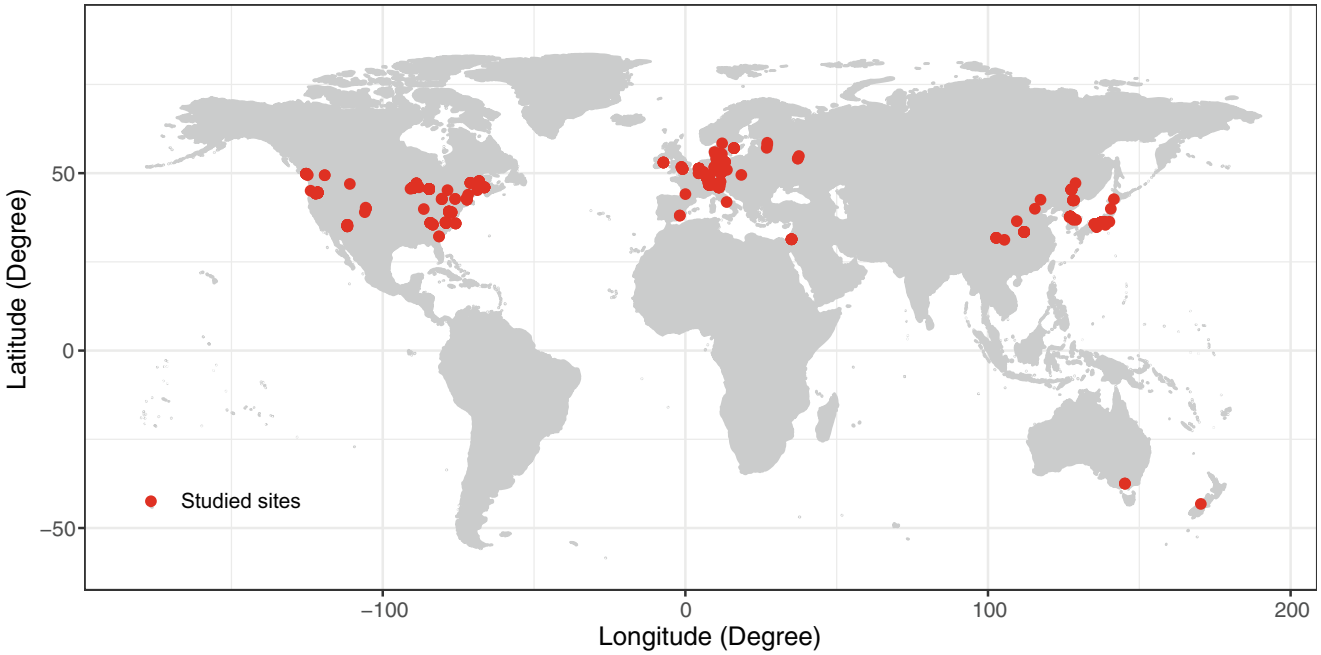

Fig. 1 Distribution of studied sites of global temperate forests compiled from the Global Soil Respiration Database (SRDB; Bond-Lamberty and Thomson 2018)

$$\mathrm{AICc} = n\log\sigma^2 + 2p + \frac{2p(p+1)}{n-p-1} \quad (1)$$

where AICc is the corrected AIC, n is the number of observations, σ is the RMSE, and p is the number of parameters.

Because the age and LAI data are not evenly distributed (with less data for high LAI values and older forests), we used the Cook's distance of a data point, denoted Di, to assess if the data point is highly influential (Cook 1977). Generally, a data point with Di > 1 is considered a highly influential point, namely an outlier (Cook and Weisberg 1982). And the outlier data point will be removed.

Results and discussion

Pattern of LAI with forest age

The pattern of LAI for global temperate forest ecosystems with age agreed with a nonlinear model consisting of a second-degree polynomial function and a Gaussian function, i.e., following a stand-replacing disturbance, LAI initially increased rapidly, reached a peak at juvenility, followed by a slow decrease until maturity, and then a possible increase with further forest aging ($R^2 = 0.21$, $P < 0.001$, Fig. 2). The fitted model was highly statistically significant (t test and F test) but exhibited a relatively low R^2. The low R^2 value was expected given the strong dependence of LAI on other factors such as climate, soil fertility, water supply, and growth density (Gholz 1982; Joggi et al. 1983; Maass et al. 1995). Although the LAI values from old forests (age > 250 y) are limited, they are important points in the regression line. Because these points were not highly influential (Di > 1), and were within the 95% confidence interval of the regression. Nonetheless, we are aware that the parameters of the model may change if we have more data, especially for older forests.

In global temperate forest ecosystems, the fitted nonlinear regression model showed an increase in LAI during the early stages of stand development, where may be due to increased nutrient availability resulting from the breakdown of woody

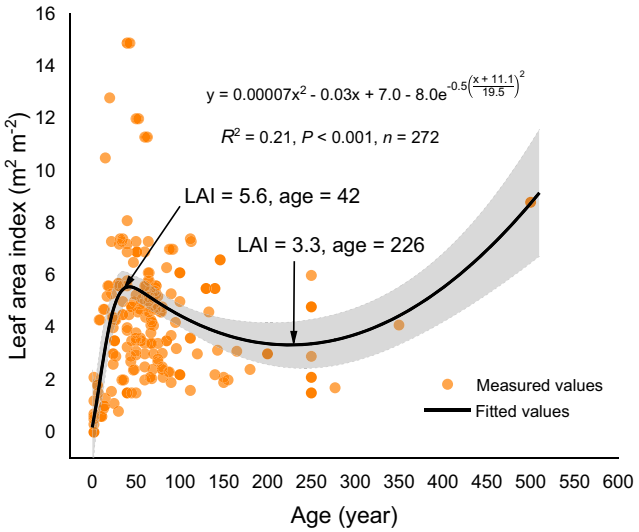

Fig. 2 The leaf area index (LAI) pattern with age across global temperate forest ecosystems. The orange solid circles indicate measurements from paired LAI-age data. The solid black line is fitted from measurement data. The gray shading indicates the 95% confidence interval of the fitted LAI

material from the previous generation (Allen et al. 1997; Clinton et al. 2002). The maximum LAI of 5.6 m^2 m^{-2} (5.1–6.1 m^2 m^{-2}, 95% confidence interval) was reached at an age of approximately 42 years. After this peak, LAI decreased gradually to 3.3 m^2 m^{-2} (2.5–4.2 m^2 m^{-2}, 95% confidence interval) at an age of approximately 226 years due to possible intraspecific competition-related mortality or self-thinning (Holdaway et al. 2008) and a probable reduction in nutrient availability (Allen et al. 1990). Over 226 years, the intraspecific competition may no longer occur when natural forests reach their equilibrium point. Subsequently, it is possible that the LAI increased gradually with forest growth. There are two possible reasons why the LAI increased in older stands. First, the breakdown of dead woody material resulting from the self-thinning mentioned above can increase nutrient availability, which leads to an increase in LAI in older stands. Second, in older stands, increased vertical stratification can improve light penetration, which also leads to an increase in LAI (Kitajima et al. 2005; Holdaway et al. 2008).

Patterns of GPP and NPP with increase in LAI

Although the changes in GPP and NPP with forest age in our dataset were fitted with the gamma (Γ) function proposed by Tang et al. (2014), the fitted Γ functions exhibited a relatively low R^2 ($R^2 = 0.16$ for GPP in Fig. S2a; $R^2 = 0.24$ for NPP in Fig. S2b). Therefore, the Γ function does not seem to be an accurate and efficient model to describe global temperate forest dynamics. We found that similar to LAI, the pattern of GPP across global temperate forest ecosystems with age agreed with the nonlinear model consisting of a linear function and a Gaussian function. The fitted model was highly statistically significant (*t* test and *F* test), and exhibited higher R^2 ($R^2 = 0.39$, Fig. 3a) and better overall performance (lower corrected AIC) than the Γ function. The pattern of GPP within 0–117 years of the forest age followed the pattern assumed in the classical model, i.e., following a stand-replacing disturbance, GPP initially increased rapidly, reached a peak at 1876 g C m^{-2} y^{-1} (1612–2139 g C m^{-2} y^{-1}, 95% confidence interval) at approximately 52 years old at juvenility, and then decreased sharply until maturity (Fig. 3a). However, over 117 years, it was possible that the field observation of GPP increased gradually with further forest aging (Fig. 3a), which does not follow the pattern hypothesized in the classical model. The pattern of NPP across global temperate forest ecosystems with age agreed with a Gaussian model. The fitted model was highly statistically significant (*t* test and *F* test), and exhibited a R^2 value ($R^2 = 0.24$, Fig. 3b) similar to the Γ function and better overall performance (lower corrected AIC). The pattern of NPP with age in the present study was consistent with the assumption by Kira and Shidei (1967), i.e., following a stand-replacing disturbance, NPP initially increased rapidly, reached a peak at juvenility, and then decreased with further

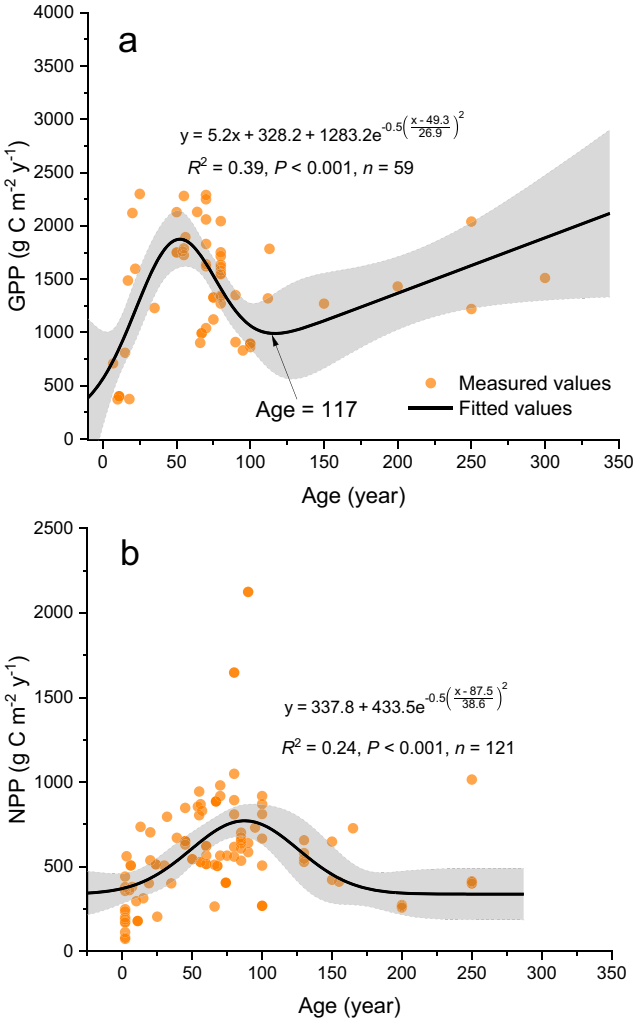

Fig. 3 Forest production patterns with age across global temperate forest ecosystems fitted by our proposed models: **a** gross primary production (GPP); **b** net primary production (NPP). The orange solid circles indicate measurements from paired data. The solid black lines are fitted from measurement data. The gray shading indicates the 95% confidence interval of fitted values

forest aging (Fig. S1). The fitted regression model showed a maximum NPP at 771 g C m^{-2} y^{-1} (676–867 g C m^{-2} y^{-1}, 95% confidence interval) at an age of approximately 87 years.

The similar trends of GPP and LAI with forest age (Figs. 2 and 3a) indicate that forest GPP should be proportional to LAI. And we found that a power function ($R^2 = 0.64$, $P < 0.001$) as opposed to a linear function can better describe the relationship between forest GPP and LAI (Fig. 4a). In the power model, 64% of GPP variance could be explained by LAI, indicating that LAI, an important structural property of vegetation, has a large effect on GPP. In the LAI range of 0–5.6 m^2 m^{-2}, the LAI of trees increases with increasing leaf area, which results in an increase in the fraction of absorbed photosynthetically active radiation (Jung et al. 2007). The increase in the fraction of absorbed photosynthetically active radiation promotes an increase in the absorbed photosynthetically active radiation by vegetation per unit time, as

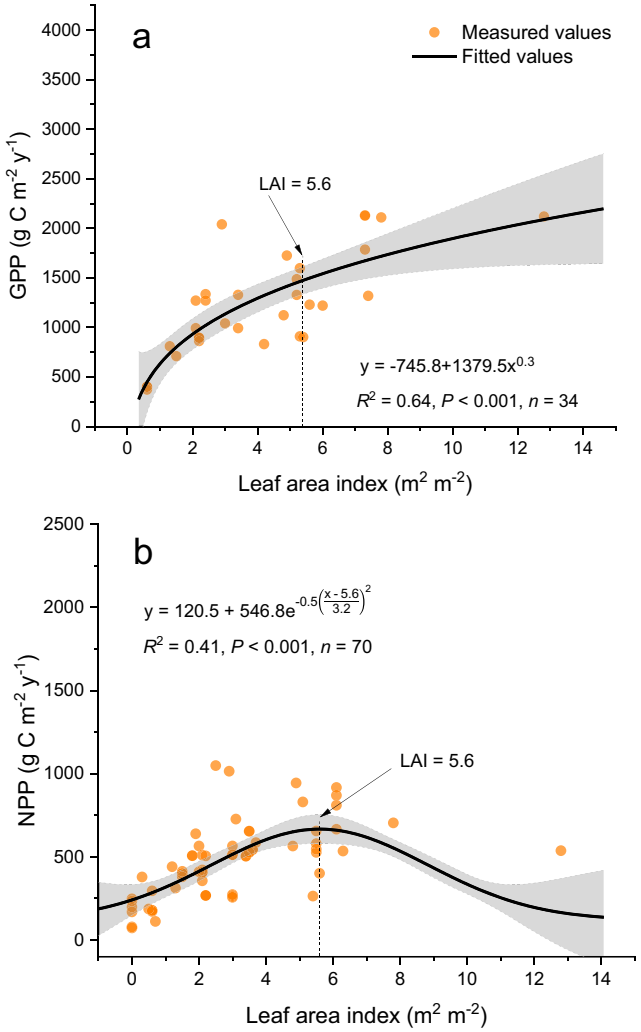

Fig. 4 Forest production patterns with increasing leaf area index (LAI) across global temperate forest ecosystems: **a** gross primary production (GPP); **b** net primary production (NPP). The orange solid circles indicate measurements from paired data. The solid black lines are fitted from measurement data. The gray shading indicates the 95% confidence interval of fitted values

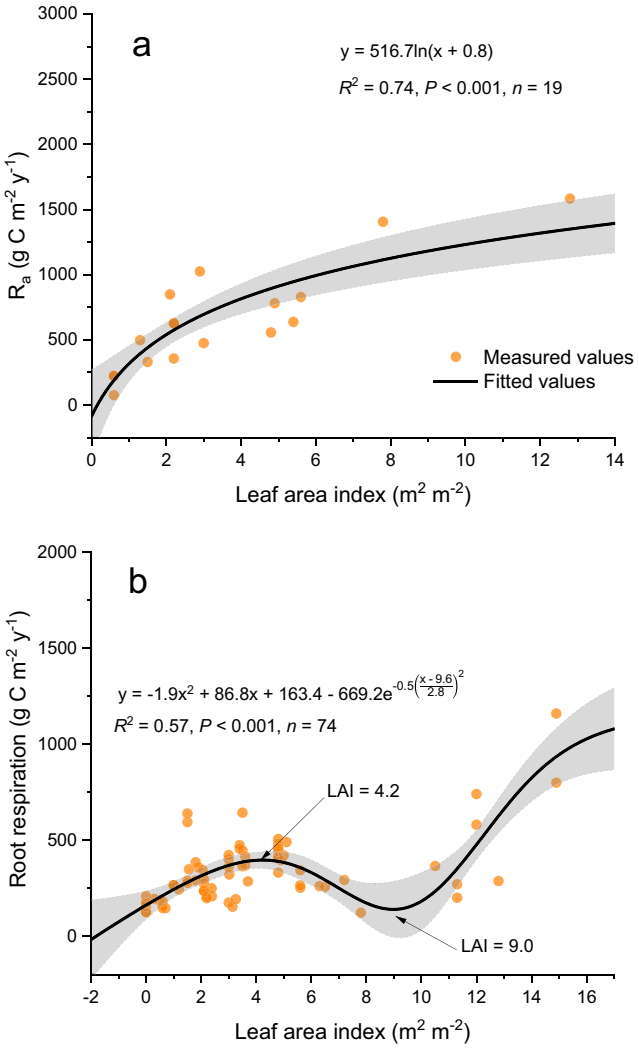

Fig. 5 Forest respiration patterns with increasing leaf area index (LAI) across global temperate forest ecosystems: **a** autotrophic respiration (R_a), the orange solid circles indicate the calculated paired R_a-LAI data (R_a is the difference between GPP and NPP); **b** root respiration, the orange solid circles indicate measurements from paired data. The solid black lines are fitted from measurement data. The gray shading indicates the 95% confidence interval of fitted values

the absorbed photosynthetically active radiation is the product of incident photosynthetically active radiation and the fraction of absorbed photosynthetically active radiation. Moreover, an increase in absorbed photosynthetically active radiation leads to an increase in GPP, as GPP is proportional to absorbed photosynthetically active radiation (Propastin et al. 2012). Accordingly, GPP increases with increasing LAI. With LAI increasing further (> 5.6 m^2 m^{-2}; Fig. 2), an asymptotic relationship between fractions of absorbed photosynthetically active radiation and LAI results in approaching saturation of photosynthetically active radiation absorbed by vegetation per unit time (Propastin et al. 2012). The possible LAI value at saturated canopy light absorption found in our study is 5.6 m^2 m^{-2} (Fig. 2), which is close to that obtained in the study by Asner et al. (2003). Saturated canopy light absorption leads to slight changes in vegetation GPP. Therefore, the LAI, an important canopy-structure parameter (Running and Coughlan 1988), is one of the determinants of forest GPP.

The relationship between NPP and LAI was characterized better by a Gaussian model ($R^2 = 0.41$, $P < 0.001$) than by other models (for example, logarithmic function, polynomial function, exponential function, and Γ function) based on the lower AIC value. NPP initially increased and subsequently decreased with increasing LAI and peaked at a LAI of approximately 5.6 m^2 m^{-2} (Fig. 4b). NPP depends on the difference between carbon assimilation by photosynthesis and carbon efflux by respiration. Based on the fluctuating trend of root respiration with the increase in LAI (Fig. 5b), the balance between

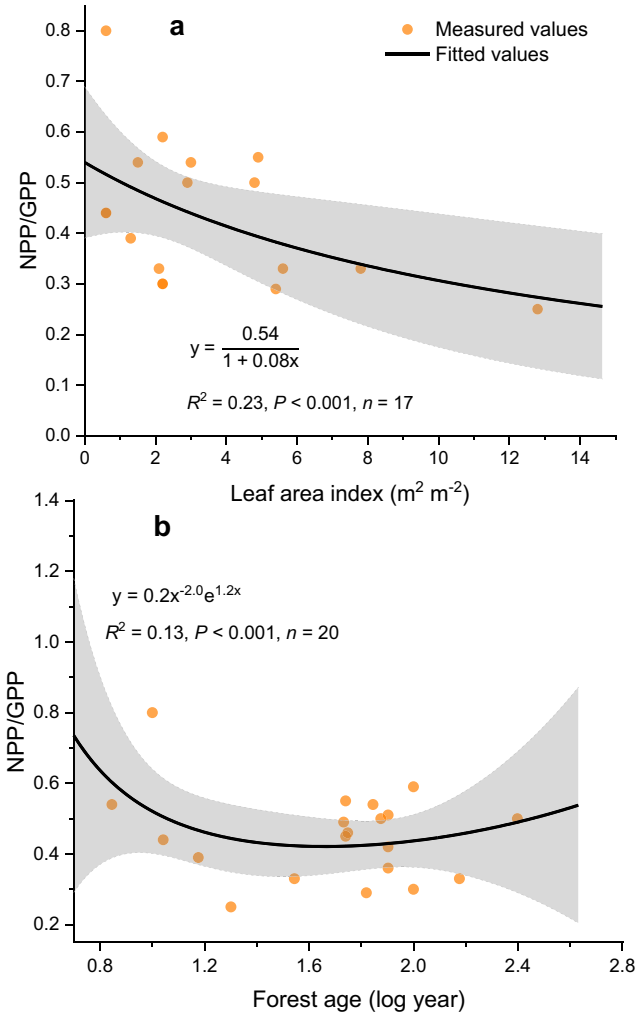

Fig. 6 The changes in the ratio NPP/GPP with leaf area index (**a**) and age (**b**) across global temperate forest ecosystems. The orange solid circles indicate measurements from paired data. The solid black lines are fitted from measurement data. The gray shading indicates the 95% confidence interval of fitted values

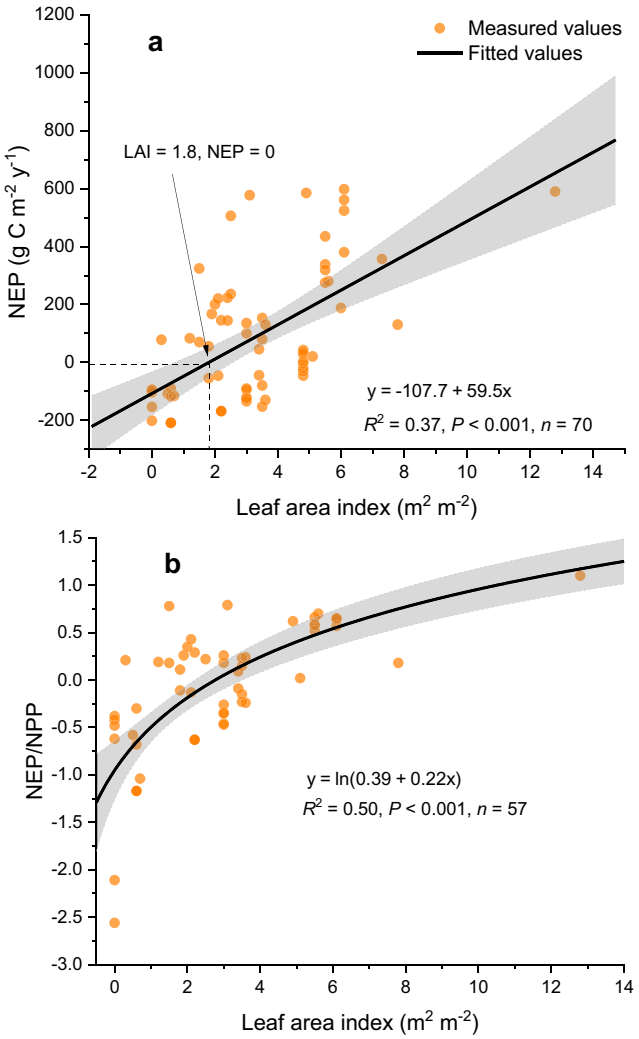

Fig. 7 The changes in NEP (**a**) and NEP/NPP (**b**) with increasing leaf area index across global temperate forest ecosystems. The orange solid circles indicate measurements from paired data. The solid black lines are fitted from data. The gray shading indicates the 95% confidence interval of fitted values

photosynthesis and respiration is discussed in three stages of 0–4.2, 4.2–9.0, and > 9.0 m^2 m^{-2}. In a LAI range of 0–4.2 m^2 m^{-2}, the soil water content and nutrients may be relatively sufficient, which results in an increase in vegetation biomass (Gower et al. 1996). The increase in foliar biomass, an important component of vegetation biomass, indicates the increase in LAI, which promotes the increase in vegetation GPP by photosynthesis, as discussed above. On the other hand, autotrophic respiration, including foliage, wood, and root respiration, will consume a large proportion of GPP (Kira and Shidei 1967). Leaf respiratory consumption is proportional to leaf biomass (Kira and Shidei 1967). And the increase in total leaf biomass results in total leaf area increasing as a power function (Holdaway et al. 2008). Thus, leaf respiration will increase with increasing LAI. Wood respiration continues to increase with the accumulation of woody biomass (Kira and Shidei 1967) and woody biomass is proportional to leaf biomass as proposed by Jenkins et al. (2003), which results in an increase in wood respiration with increasing LAI. Root respiration depends largely on tree photosynthesis (Högberg et al. 2001). An increase in photosynthesis caused by higher LAI can supply more products for root growth and maintenance. An increase in root production promotes an increase in root respiration (Wang and Yang 2007). Accordingly, the autotrophic respiration, the sum of leaf, wood, and root respiration, increases with an increase in LAI. Because the rate of autotrophic respiration is lower than the rate of GPP with increasing LAI in the 0–4.2 m^2 m^{-2} LAI range (Figs. 4a and 5a), the resulting NPP, which is the difference between GPP and autotrophic respiration, increases with an increase in LAI. Our fitting curve in the 0–4.2 m^2 m^{-2} LAI range for the relationship between NPP and leaf area index is close to the reported linear relationship between these two variables in the literature (Kassnacht and Gower 1997; Bolstad et al. 2000; Kushida et al. 2007).

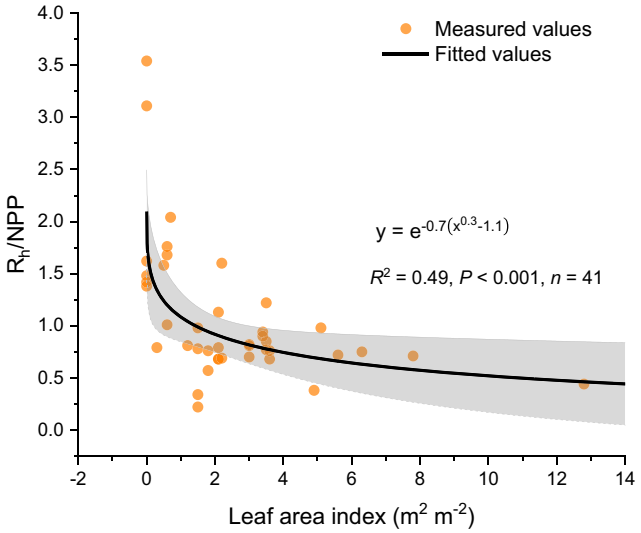

Fig. 8 The change in ratio of heterotrophic respiration to net primary production (R_h/NPP) with increasing leaf area index across global temperate forest ecosystems. The orange solid circles indicate measurements from paired R_h-NPP data. The solid black line is fitted from measurement data. The gray shading indicates the 95% confidence interval of fitted values

Over the LAI range of 4.2–9.0 m^2 m^{-2}, leaf and wood respiration continue to increase, but root respiration exhibited a decreasing trend with increasing LAI (Fig. 5b). The decrease in root respiration results from forest canopy closure. The canopy closure will decrease net radiation on the forest floor and subsequently lower soil temperature with increasing LAI (Tanaka and Hashimoto 2006). The lowered soil temperature leads to a decrease in root respiration (Boone et al. 1998). Although root respiration has a decreasing trend with increasing LAI, the increment in aboveground plant respiration (the sum of leaf and wood respiration) is far greater than the decrement in root respiration. Therefore, autotrophic respiration exhibited an increasing trend with increasing LAI (Fig. 5a). On the other hand, the vegetation GPP slightly increased with increasing LAI (Fig. 4a). This is because when the LAI value exceeds 4.2 m^2 m^{-2}, the forest will form gradually a closed canopy, which leads to approaching saturation of the light absorption of vegetation (Asner et al. 2003). Accordingly, the resulting NPP decreases with increasing LAI.

After the LAI value reaches 9.0 m^2 m^{-2}, the dense leaf area of the canopy results in higher canopy transpiration rates. The high transpiration leads to limited soil moisture. Although limited soil moisture inhibits canopy photosynthesis, evolutionary adaptations, including increased leaf stomatal density (Xu and Zhou 2008), decreased leaf stomatal size (Xu and Zhou 2008), greater leaf thickness (Galmés et al. 2007; Giuliani et al. 2013), and increased leaf venation (Xu et al. 2009), arise to increase water use efficiency and light-utilization efficiency to promote photosynthesis. The adaptation of morphological traits results in a steady-state GPP. On the other hand, leaf and wood respiration continue to increase with increasing LAI. Soil water limitation causes root growth, especially fine root growth, to increase water uptake to compensate for transpiration loss (Kozlowski and Pallardy 2002; Metcalfe et al. 2008). The resulting root growth increases root respiration. The resulting autotrophic respiration (the sum of leaf, wood, and root respiration) increases with an increase in LAI. Considering that GPP is in steady-state as LAI is more than 9.0 m^2 m^{-2}, NPP shows a decreasing trend with the increase in LAI.

Variation in NPP/GPP and NEP/NPP ratios with increasing LAI

We found that the NPP/GPP ratio significantly decreased in response to the increase in leaf area index across global temperate forest ecosystems ($R^2 = 0.23$, $P < 0.001$, Fig. 6a). The decrease in NPP/GPP ratio results from the increase in LAI-driven autotrophic respiration (NPP/GPP = 1—R_a/GPP). In addition, we also found NPP/GPP ratio also was not constant with forest aging but initially decreased and subsequently increased within the forest age range of 0–250 years ($R^2 = 0.13$, $P < 0.001$, Fig. 6b). Our results suggest that a constant ratio of NPP to GPP is possibly problematic in some carbon balance models.

Net ecosystem production (NEP) increased linearly with increasing LAI ($R^2 = 0.37$, $P < 0.001$, Fig. 7a). NEP was negative when LAI was less than 1.8 m^2 m^{-2}, indicating a source of carbon for the atmosphere. During disturbance, live biomass decreases and the amount of carbon in the plant debris increases. Following the disturbance, this detritus subsequently decomposes, resulting in declining detrital stocks and a high heterotrophic respiration (R_h). On the other hand, the increase in the leaf area index of plants leads to a recovery in production, which results in a gradual increase in live biomass. However, the loss of detritus is more rapidly than the accumulation of live biomass, resulting in an initial loss of total carbon and driving the net efflux of carbon dioxide to the atmosphere (Goulden et al. 2011). When LAI > 1.8 m^2 m^{-2}, NEP was positive, indicating a carbon sink. This is because plant growth and biomass accumulation increase, and decomposition rate of plant litter is lower than the accumulation rate of litter, which leads to the increase in carbon accumulation with increasing LAI (Goulden et al. 2011). In addition, we found that the NEP/NPP ratio logarithmically increased with the increase in LAI ($R^2 = 0.50$, $P < 0.001$, Fig. 7b), which is primarily caused by the decrease in the R_h/NPP ratio with increasing LAI ($R^2 = 0.49$, $P < 0.001$, Fig. 8; NEP/NPP = 1—R_h/NPP).

A Gaussian function can describe well the change in NPP with plant carbon production efficiency (the ratio of NPP to GPP) for global temperate forest ecosystems ($R^2 = 0.38$, $P < 0.01$, Fig. 9a). And NPP peaked at the ratio NPP/GPP of about 0.5. This may be because with LAI increasing,

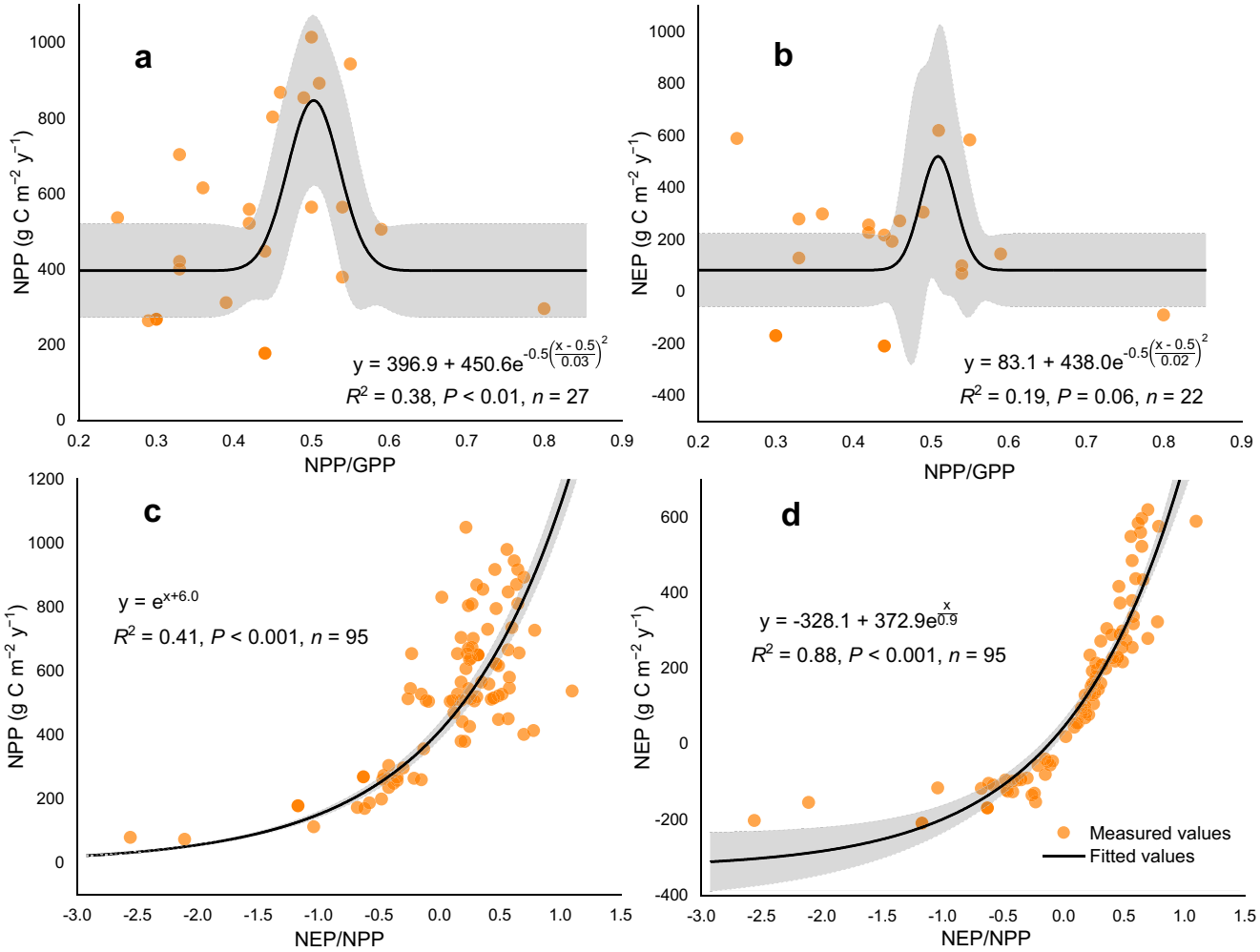

Fig. 9 The changes in NPP and NEP with the ratios of NPP/GPP and NEP/NPP across global temperate forest ecosystems. The orange solid circles indicate measurements from paired data. The solid black line is fitted from measurement data. The gray shading indicates the 95% confidence interval of fitted values

photosynthesis (GPP) increases firstly and then approaches saturation, and autotrophic respiration increases continuously; when autotrophic respiration accounts for 50% of GPP (the ratio NPP/GPP is about 0.5), NPP may reach maximum value. The change in NEP with the ratio NPP/GPP was similar to that of NPP (R^2 = 0.19, P = 0.06, Fig. 9b) due to the positive correlation between NEP and NPP (Waring and Running 2007). In addition, NPP and NEP increased exponentially with the ratio of NEP/NPP (R^2 = 0.41, P < 0.001, Fig. 9c for NPP and R^2 = 0.88, P < 0.001, Fig. 9d for NEP), which indicates that a small increase in plant carbon storage efficiency (NEP/NPP) will promote a large carbon sequestration.

Conclusions

Here, we proposed an empirical nonlinear model consisting of a polynomial function and a Gaussian function to determine the dynamics of LAI with forest age across global natural temperate forest ecosystems. The model indicated that LAI initially increased rapidly, reached a peak at juvenility, decreased slowly until maturity, and again increased possibly with further forest aging following a stand-replacing disturbance. We found that a Gaussian function with/without a linear function was appropriate to describe the patterns of GPP and NPP for global temperate forest ecosystems with age. We found that the dynamics of GPP across global temperate forest ecosystems was driven by LAI. GPP initially increased and subsequently stabilized with increasing LAI. Moreover, the dynamics of NPP across global temperate forest ecosystems was also driven by LAI. NPP peaked at LAI of about 5.6 m^2 m^{-2}, and subsequently decreased. We specified that the LAI-driven unimodal pattern of NPP resulted from the combined effects of (1) an increase and subsequent steady GPP with increasing LAI and (2) a continuing decrease in the NPP/GPP ratio with increasing LAI, i.e., R_a increased significantly with increasing LAI, and especially after canopy closure, R_a increased more quickly with increasing LAI than GPP. In addition, following a stand-replacing disturbance, NEP increased

linearly with increasing LAI. Understanding the control of LAI on ecosystem production contributes to predict long-term ecosystem responses to global change for making sound climate change policies. As a limitation of our investigation, more study sites, recording forest production and leaf area index, need to be included for a better understanding of LAI-driven patterns of global temperate forest production.

Supplementary Information The online version contains supplementary material available at https://doi.org/10.1007/s11356-020-11928-0.

Acknowledgments This work was funded jointly by the National Natural Science Foundation of China (Nos. 41877037, 41425006, and 41101218), and the Western Light Project of Chinese Academy of Sciences (No. K318001103). The authors thank B. Bond-Lamberty for making available the comprehensive soil respiration database including plant primary production data.

Authors' contributions W.Z. analyzed the data. W.Z., W.F.T., and S.Q.L. contributed to the discussion of the results and wrote the paper.

Funding The National Natural Science Foundation of China (Nos. 41877037, 41425006, and 41101218), the Western Light Project of Chinese Academy of Sciences (No. K318001103).

Data availability Not applicable.

Compliance with ethical standards

Competing interests The authors declare that they have no competing interests.

Ethics approval and consent to participate Not applicable.

Consent for publication Not applicable.

References

Allen HL, Dougherty PM, Campbell RG (1990) Manipulation of water and nutrients — practice and opportunity in southern U.S. pine forests. For Ecol Manag 30:437–453

Allen RB, Clinton PW, Davis MR (1997) Cation storage and availability along a Nothofagus forest development sequence in New Zealand. Can J For Res 27:323–330

Asner GP, Scurlock JMO, Hicke JA (2003) Global synthesis of leaf area index observations: implications for ecological and remote sensing studies. Glob Ecol Biogeogr 12:191–205

Bolstad PV, Vose JM, McNulty SG (2000) Forest productivity, leaf area, and terrain in southern appalachian deciduous forests. For Sci 47:419–427

Bondeau A, Kicklighter DW, Kaduk J, Intercomparison T, Participants, OF., ThE., Potsdam, NpP., Model (1999) Comparing global models of terrestrial net primary productivity (NPP): importance of vegetation structure on seasonal NPP estimates. Glob Chang Biol 5:35–45

Bond-Lamberty BP, Thomson AM (2018) A global database of soil respiration data, Version 4.0, in, ORNL Distributed Active Archive Center

Boone RD, Nadelhoffer KJ, Canary JD, Kaye JP (1998) Roots exert a strong influence on the temperature sensitivity of soil respiration. Nature 396:570–572

Clinton PW, Allen RB, Davis MR (2002) Nitrogen storage and availability during stand development in a New Zealand Nothofagus forest. Can J For Res 32:344–352

Cook RD (1977) Detection of influential observation in linear regression. Technometrics 19:15–18

Cook RD, Weisberg S (1982) Residuals and influence in regression. Chapman & Hall, New York

da Silva DA, Pfeifer M, Pattison Z, Vibrans AC (2020) Drivers of leaf area index variation in Brazilian Subtropical Atlantic Forests. For Ecol Manag 476:118477

de Almeida CL, de Carvalho TRA, de Araújo JC (2019) Leaf area index of Caatinga biome and its relationship with hydrological and spectral variables. Agric For Meteorol 279:107705

Drake JE, Davis SC, Raetz LM, DeLucia EH (2011) Mechanisms of age-related changes in forest production: the influence of physiological and successional changes. Glob Chang Biol 17:1522–1535

Fotis AT, Morin TH, Fahey RT, Hardiman BS, Bohrer G, Curtis PS (2018) Forest structure in space and time: biotic and abiotic determinants of canopy complexity and their effects on net primary productivity. Agric For Meteorol 250-251:181–191

Galmés J, Flexas J, Savé R, Medrano H (2007) Water relations and stomatal characteristics of Mediterranean plants with different growth forms and leaf habits: responses to water stress and recovery. Plant Soil 290:139–155

Gholz HL (1982) Environmental limits on aboveground net primary production, leaf area, and biomass in vegetation zones of the Pacific northwest. Ecology 63:469–481

Giuliani R, Koteyeva N, Voznesenskaya E, Evans MA, Cousins AB, Edwards GE (2013) Coordination of leaf photosynthesis, transpiration, and structural traits in rice and wild relatives (genus *Oryza*). Plant Physiol 162:1632–1651

Goulden ML, McMillan AMS, Winston GC, Rocha AV, Manies KL, Harden JW, Bond-Lamberty BP (2011) Patterns of NPP, GPP, respiration, and NEP during boreal forest succession. Glob Chang Biol 17:855–871

Gower ST, Vogt KA, Grier CC (1992) Carbon dynamics of rocky mountain douglas-fir: influence of water and nutrient availability. Ecol Monogr 62:43–65

Gower ST, McMurtrie RE, Murty D (1996) Aboveground net primary production decline with stand age: potential causes. Trends Ecol Evol 11:378–382

Han T, Ren H, Wang J, Lu H, Song G, Chazdon RL (2020) Variations of leaf eco-physiological traits in relation to environmental factors during forest succession. Ecol Indic 117:106511

He L, Chen JM, Pan Y, Birdsey R, Kattge J (2012) Relationships between net primary productivity and forest stand age in U.S. forests. Glob. Biogeochem Cycles 26:GB3009

Högberg P, Nordgren A, Buchmann N, Taylor AFS, Ekblad A, Högberg MN, Nyberg G, Ottosson-Löfvenius M, Read DJ (2001) Large-scale forest girdling shows that current photosynthesis drives soil respiration. Nature 411:789–792

Holdaway RJ, Allen RB, Clinton PW, Davis MR, Coomes DA (2008) Intraspecific changes in forest canopy allometries during self-thinning. Funct Ecol 22:460–469

Jenkins JC, Chojnacky DC, Heath LS, Birdsey RA (2003) National-scale biomass estimators for United States tree species. For Sci 49:12–35

Joggi D, Hofer U, Nösberger J (1983) Leaf area index, canopy structure and photosynthesis of red clover (Trifolium pratense L.). Plant, Cell Environ 6:611–616

Jung M, Le Maire G, Zaehle S, Luyssaert S, Vetter M, Churkina G, Ciais P, Viovy N, Reichstein M (2007) Assessing the ability of three land ecosystem models to simulate gross carbon uptake of forests from boreal to Mediterranean climate in Europe. Biogeosciences 4:647–656

Kashian DM, Romme WH, Tinker DB, Turner MG, Ryan MG (2013) Postfire changes in forest carbon storage over a 300-year

chronosequence of Pinus contorta-dominated forests. Ecol Monogr 83:49–66

Kassnacht KS, Gower ST (1997) Interrelationships among the edaphic and stand characteristics, leaf area index, and aboveground net primary production of upland forest ecosystems in north Central Wisconsin. Can J For Res 27:1058–1067

Kira T, Shidei T (1967) Primary production and turnover of organic matter in different forest ecosystems of the western pacific. Jpn J Ecol 17:70–87

Kitajima K, Mulkey SS, Wright SJ (2005) Variation in crown light utilization characteristics among tropical canopy trees. Ann Bot 95:535–547

Kozlowski TT, Pallardy SG (2002) Acclimation and adaptive responses of woody plants to environmental stresses. Bot Rev 68:270–334

Kulmala L, Pumpanen J, Kolari P, Dengel S, Berninger F, Köster K, Matkala L, Vanhatalo A, Vesala T, Bäck J (2019) Inter- and intra-annual dynamics of photosynthesis differ between forest floor vegetation and tree canopy in a subarctic Scots pine stand. Agric For Meteorol 271:1–11

Kushida K, Isaev AP, Maximov TC, Takao G, Fukuda M (2007) Remote sensing of upper canopy leaf area index and forest floor vegetation cover as indicators of net primary productivity in a Siberian larch forest. Journal of Geophysical Research: Biogeosciences 112:G02003

Lee H, Park J, Cho S, Lee M, Kim HS (2019) Impact of leaf area index from various sources on estimating gross primary production in temperate forests using the JULES land surface model. Agric For Meteorol 276-277:107614

Levenberg K (1944) A method for the solution of certain non-linear problems in least squares. Q Appl Math 2:164–168

Li L, Chen S, Yang C, Meng F, Sigrimis N (2020) Prediction of plant transpiration from environmental parameters and relative leaf area index using the random forest regression algorithm. J Clean Prod 261:121136

Lourakis M (2005) A brief description of the Levenberg-Marquardt algorithm implemened by levmar. Foundation of Research and Technology 4:1–6

Luyssaert S, Inglima I, Jung M, Richardson AD, Reichstein M, Papale D, Piao SL, Schulze E-D, Wingate L, Matteucci G, Aragao L, Aubinet M, Beer C, Bernhofer C, Black KG, Bonal D, Bonnefond J-M, Chambers J, Ciais P, Cook B, Davis KJ, Dolman AJ, Gielen B, Goulden M, Grace J, Granier A, Grelle A, Griffis T, Gr Nwald T, Guidolotti G, Hanson P, Harding R, Hollinger DY, Hutyra LR, Kolari P, Kruijt B, Kutsch W, Lagergren F, Laurila T, Law B, Le Maire G, Lindroth A, Loustau D, Malhi Y, Mateus J, Migliavacca M, Misson L, Montagnani L, Moncrieff J, Moors E, Munger JW, Nikinmaa E, Ollinger S, Pita G, Rebmann C, Roupsard O, Saigusa N, Sanz M, Seufert G, Sierra C, Smith M-L, Tang J, Valentini R, Vesala T, Janssens IA (2007) CO_2 balance of boreal, temperate, and tropical forests derived from a global database. Glob Chang Biol 13:2509–2537

Luyssaert S, Schulze ED, Börner A, Knohl A, Hessenmöller D, Law BE, Ciais P, Grace J (2008) Old-growth forests as global carbon sinks. Nature 455:213–215

Maass J, Vose JM, Swank WT, Martínez-Yrízar A (1995) Seasonal changes of leaf area index (LAI) in a tropical deciduous forest in west Mexico. For Ecol Manag 74:171–180

Marquardt DW (1963) An algorithm for least-squares estimation of nonlinear parameters. J Soc Ind Appl Math 11:431–441

Metcalfe DB, Meir P, Aragão LEOC, da Costa ACL, Braga AP, Gonçalves PHL, de Athaydes Silva Junior J, de Almeida SS, Dawson LA, Malhi Y, Williams M (2008) The effects of water availability on root growth and morphology in an Amazon rainforest. Plant Soil 311:189–199

Migliavacca M, Sonnentag O, Keenan TF, Cescatti A, O'Keefe J, Richardson AD (2012) On the uncertainty of phenological responses to climate change, and implications for a terrestrial biosphere model. Biogeosciences 9:2063–2083

Parker GG (2020) Tamm review: leaf area index (LAI) is both a determinant and a consequence of important processes in vegetation canopies. For Ecol Manag 477:118496

Pregitzer KS, Euskirchen ES (2004) Carbon cycling and storage in world forests: biome patterns related to forest age. Glob Chang Biol 10: 2052–2077

Propastin P, Ibrom A, Knohl A, Erasmi S (2012) Effects of canopy photosynthesis saturation on the estimation of gross primary productivity from MODIS data in a tropical forest. Remote Sens Environ 121:252–260

Running SW, Coughlan JC (1988) A general model of forest ecosystem processes for regional applications I. Hydrologic balance, canopy gas exchange and primary production processes. Ecol Model 42:125–154

Ryan MG, Binkley D, Fownes JH (1997) Age-related decline in forest productivity: pattern and process. In: Begon M, Fitter AH (eds) . Academic Press, Adv Ecol Res, pp 213–262

Ryan MG, Binkley D, Fownes JH, Giardina CP, Senock RS (2004) An experimental test of the causes of forest growth decline with stand age. Ecol Monogr 74:393–414

Sellers PJ, Hall FG, Asrar G, Strebel DE, Murphy RE (1988) The first ISLSCP field experiment (FIFE). Bull Am Meteorol Soc 69:22–27

Sellers PJ, Hall FG, Kelly RD, Black A, Baldocchi D, Berry J, Ryan M, Ranson KJ, Crill PM, Lettenmaier DP, Margolis H, Cihlar J, Newcomer J, Fitzjarrald D, Jarvis PG, Gower ST, Halliwell D, Williams D, Goodison B, Wickland DE, Guertin FE (1997) BOREAS in 1997: experiment overview, scientific results, and future directions. Journal of Geophysical Research: Atmospheres 102:28731–28769

Tanaka K, Hashimoto S (2006) Plant canopy effects on soil thermal and hydrological properties and soil respiration. Ecol Model 196:32–44

Tang J, Luyssaert S, Richardson AD, Kutsch W, Janssens IA (2014) Steeper declines in forest photosynthesis than respiration explain age-driven decreases in forest growth. Proc Natl Acad Sci U S A 111:8856–8860

Tyrrell ML, Ross J, Kelty M (2012) Carbon dynamics in the temperate forest. In: Ashton MS, Tyrrell ML, Spalding D, Gentry B (eds) Managing forest carbon in a changing climate. Springer Netherlands, Dordrecht, pp 77–107

Wales SB, Kreider MR, Atkins J, Hulshof CM, Fahey RT, Nave LE, Nadelhoffer KJ, Gough CM (2020) Stand age, disturbance history and the temporal stability of forest production. For Ecol Manag 460:117865

Wang C, Yang J (2007) Rhizospheric and heterotrophic components of soil respiration in six Chinese temperate forests. Glob Chang Biol 13:123–131

Waring RH, Running SW (2007) CHAPTER 10 - advances in Eddy-flux analyses, remote sensing, and evidence of climate change. In: Waring RH, Running SW (eds) Forest ecosystems (Third Edition). Academic Press, San Diego, pp 317–344

Xu Z, Zhou G (2008) Responses of leaf stomatal density to water status and its relationship with photosynthesis in a grass. J Exp Bot 59:3317–3325

Xu F, Guo W, Xu W, Wei Y, Wang R (2009) Leaf morphology correlates with water and light availability: what consequences for simple and compound leaves? Prog Nat Sci 19:1789–1798

Yang X, Mustard JF, Tang J, Xu H (2012) Regional-scale phenology modeling based on meteorological records and remote sensing observations Journal of Geophysical Research: Biogeosciences 117

Zha TS, Barr AG, Bernier PY, Lavigne MB, Trofymow JA, Amiro BD, Arain MA, Bhatti JS, Black TA, Margolis HA, McCaughey JH, Xing ZS, Van Rees KCJ, Coursolle C (2013) Gross and aboveground net primary production at Canadian forest carbon flux sites. Agric For Meteorol 174-175:54–64